Department of Biopharmaceutics and Pharmaceutical Technology[1], Institute of Pharmaceutical and Biomedical Science, Johannes Gutenberg-University, Mainz; Department of Dermatology and Venereology[2], Medical Faculty; Institute of Applied Dermatopharmacy[3], Martin Luther University Halle-Wittenberg, Halle (Saale), Germany

# Delivery of free amino acids into and through the stratum corneum of the skin using micro emulsions and microemulsion-based hydrogels: Formulation, characterization, and *ex-vivo* permeation studies

B. N. Kahsay[1], S. L. Meiser[1], J. Wohlrab[2], R. H.H. Neubert[3], P. Langguth[1,*]

*Received March 22, 2023, accepted July 7, 2023*

**Corresponding author: Prof. Peter Langguth, Department of Biopharmaceutics and Pharmaceutical Technology, Institute of Pharmaceutical and Biomedical Science, Johannes Gutenberg-University, Staudingerweg 5, 55099, Mainz, Germany*
*langguth@uni-mainz.de*

*Pharmazie 78: 177-184 (2023)* *doi: 10.1691/ph.2023.3011*

Free amino acids constitute the largest portion (40%) of the natural moisturizing factor. Their level might decline and cause dry skin condition. The treatment strategy involves the replenishment of these components to the skin, and, to our knowledge, there are no reports that involve dermal delivery of free amino acids. The purpose of the current study was therefore to prepare and characterize different micro-emulsions, micro-emulsion-based hydrogels, and hydrophilic creams loaded with free amino acids for dermal delivery. Oil-in-water microemulsions were prepared using carefully selected formulation components. Poloxamer® 407 and carbopol® 934 were used to prepare the hydrogels. All the formulations were characterized for physico-chemical, permeation and cytotoxicity properties. The results showed that the prepared microemulsions had desired droplet size, size distribution, zeta potential, refractive index, and pH. In the gel preparations, the elastic properties prevailed over the viscous behavior. The hydrogels had non-Newtonian shear-thinning behavior with some thixotropic properties. The free amino acids permeated into the deeper layers of the stratum corneum from the microemulsions, and microemulsion-based hydrogels as compared to conventional hydrophilic cream. The hydrogels were more effective than the microemulsions to deliver the FAAs to the desired site of the skin in a sustained manner. Poloxamer-based hydrogel permeated into deeper skin layers than Carbopol-based hydrogel. Formulations prepared using standard free amino acids and those extracted and purified from oyster mushroom had similar characteristics. All the formulations were stable and safe to be applied topically. In conclusion, microemulsions and microemulsion-based hydrogels can be considered as safe carrier systems for dermal delivery of free amino acids.

## 1. Introduction

Human skin, the largest organ of the human body in terms of surface area, is an important target site for the administration of drugs. Thus, dermal drug delivery has been an encouraging concept for a long time. This route is noninvasive and allows targeting to the pathological sites within the skin with minimal systemic exposure, for example in skin cancer, psoriasis, eczema, and microbial infections where the site of the disease is located within the skin (Brown et al. 2006).

Free amino acids (FAAs) constitute the largest component (~40%) of the natural moisturizing factors (NMF) and they are indispensable for healthy skin. These compounds are important in maintaining the moisture balance of the skin. Previous studies by Hussain et al. (2019a) indicated that there are about 23 FAAs (at different concentrations) localized in human corneocytes within the NMFs. Studies indicate that the level of NMFs including FAAs can decline in disease conditions such as atopic dermatitis, ichthyosis vulgaris, psoriasis, and age in addition to environmental conditions (Verdier-Sévrain and Bonté 2007; Kwan et al. 2012; Takada et al. 2012). The formulation strategy to overcome this problem is the delivery of these NMF components to the human skin (Arezki et al. 2017).

Like with any hydrophilic drug candidate, the key step in the dermal delivery of FAAs is to deliver them across the SC in an adequate amount to exert a therapeutic effect. This requires detailed understanding of the delivery pathway exerted by the delivery system. For example, FAAs as highly hydrophilic molecules cannot be candidates for the intercellular pathway. It is thus unlikely that these molecules are penetrating *via* the SC lipid bi-layers because of the tight structure of the lipids and the lack of water in between the lipid bi-layers. There are just a few water molecules in the SC (Bouwstra et al. 2003; Kiselev et al. 2005; Groen et al. 2011) which are forming the tight network of hydrogen bridges between the head groups of the SC lipids. Therefore, another pathway should be taken into consideration concerning the skin uptake of the FAAs. The corneocytary diffusion pathway, which is a polar pathway involving transcellular transport through corneocytes (CORs) and intercellular transport through corneodesmosomes, appears to be relevant for such small hydrophilic molecules such as the FAAs (Hussain et al. 2019 a, b).

Once the delivery pathway is known, attaining topical bioavailability of hydrophilic active substances, like FAAs and peptide-like substances is highly challenging. It requires the development of an effective topical drug delivery system intended to suitably modulate the FAAs release rate, thus prolonging skin hydration effect, and enhanced localization in the skin. Colloidal systems are suitable vehicles for dermal and transdermal delivery of drugs (Schroeter et al. 2010; Liu et al. 2011; Fanun 2009; Panseria et al. 2014). This might be attributed to the interaction of their components with the SC to reduce its diffusional barrier, their ability to increase concentration and thermodynamic activity of drugs at the site of administration, and their hydration effect on the SC (Sahle et al. 2013).

Among other colloidal systems, micro-emulsions (MEs) have been explored as an effective carrier. They are transparent, monophasic, optically isotropic, and thermodynamically stable colloidal dispersions composed of oil, water, surfactant, and co-surfactant with droplet sizes in the range 10–100 nm (Danielsson and Lindman 1981). They have been recommended as suitable drug carrier systems for both lipophilic and hydrophilic drugs (Rhee et al. 2001; El-Laithy et al. 2002; Hua et al. 2004; Azeem et al. 2009; Rozman et al. 2009). Thus, MEs are effective carrier systems to deliver polar drugs across the skin for local and systemic effects (Kaur et al. 2018; Alkrad et al. 2019; Talhouni et al. 2019; Kumbhar et al. 2020). They have larger surface area of the inner dispersed phase which gives improved penetration capacity across biological membranes, improved drug release, remarkably high active loading capacity, and high stability (Hashem et al. 2011; Sapra et al. 2014; Nastiti et al. 2017). Although research of MEs as carriers for amino acids and peptide drugs is at an early stage, it has proven to be of interest (Goebel et al. 2008, 2012; Neubert et al. 2018).
While MEs offer numerous advantages for topical delivery, it is difficult to stabilize them on the skin surface because of their low viscosity (Zhu et al. 2009). To overcome this problem, microemulsion-based hydrogels (MEBHGs) might be advantageous. These types of formulations combine the advantages of MEs and hydrogels. To the best of our knowledge, no work has been done on the dermal delivery of FAAs using colloidal carrier systems. Therefore, the aim of this study was to develop and characterize novel FAA-loaded oil-in-water MEs and MEBHGs that could improve the bioavailability of FAAs in the skin through their dermal delivery. As reported in our previous work (Kahsay et al. 2021), FAAs for pharmaceutical or cosmeceutical purposes can be obtained from a single source (plant or fungi) and oyster mushroom had the highest content of FAAs than the other plants. Hence, formulations were prepared using the crude extracts obtained from oyster mushroom and those standard FAA mixtures.

## 2. Investigations and results

### *2.1. Formulation and characterization of MEs containing FAAs*

After selecting the desired formulation ingredients, the MEs were prepared and characterized as per the procedure outlined in the experimental section. The physico-chemical and particle properties of the MEs are shown in Table 1. Droplet sizes and polydispersity indexes (PDI) for all formulations were in the range of 17.43 to 37.40 nm and 0.0.04 to 0.18, respectively. The zeta potential ranged from -0.53 to -3.51 and the viscosities were in the range of 44.40 to 66.23 cp. While the refractive indexes and the pH values for the four MEs were not significantly different ($p > 0.05$), the globule sizes and viscosities of the three MEs (ME1, ME2, ME3) were significantly different ($p < 0.05$). ME1 and ME4 had the same formulation components (except for the source of the FAAs) and they showed almost identical characteristics.

No precipitation, phase separation or color changes were observed after the MEs were subjected to the three stress tests (heating-cooling cycle, centrifugation, and freeze-thaw cycle) indicating that the MEs were thermodynamically stable. Moreover, all MEs were stable over a period of one year (no evidence of precipitation, crystallization, color change and phase separation).

### *2.2. Rheology test for MEBHGs*

In the rheology test for the gel formulations, first, strain sweep measurements were made. The formulations showed linear deformation behavior (i.e., moduli were independent of the strain amplitude) below ca. 10 % and a strong decrease in modulus (shear thinning behavior) above the critical strain level (non-linear range). Below the critical strain level, the structure of the gel formulations was intact, they behave solid-like, and storage modulus (G') was greater than loss modulus (G''). Based on this preliminary test, a deformation amplitude of 1 % was selected for the next frequency sweep (i.e., measurement with varying frequency at fixed amplitude) in the linear viscoelastic range (LVR) from which the storage modulus G' and loss modulus G'' were obtained as shown in Fig. 1.

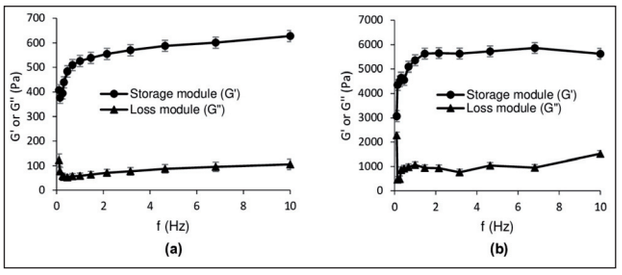


Fig. 1: Frequency sweep for the gel formulations (storage module (G') and loss module (G'') as a function of angular frequency (f) at 1% strain measured at 32 °C ((a) MEBHG1, (b) MEBHG2).

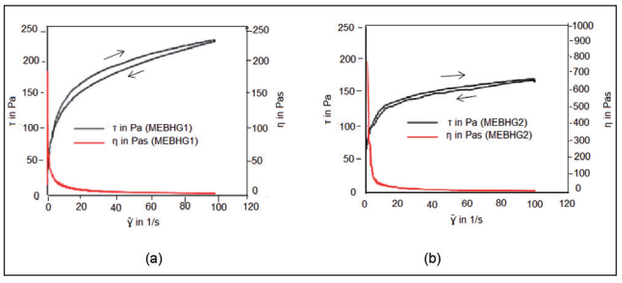


Fig. 2: Hysteresis loop of the gel formulations (shear stress as a function of controlled shear rate) and viscosity as a function of shear rate measured at 32 °C. ((a) MEBHG1, (b) MEBHG2).

**Table 1: Physico-chemical and particle properties of the different formulations (n=3, mean ± SD)**

| Parameter | Formulation code | | | |
|---|---|---|---|---|
| | ME1 | ME2 | ME3 | ME4 |
| Globule size (nm) | 17.43 ± 0.26 | 25.65 ± 0.40 | 37.40 ± 0.24 | 20.51 ± 0.09 |
| Polydispersity index (PDI) | 0.18 ± 0.02 | 0.13 ± 0.01 | 0.14 ± 0.03 | 0.04 ± 0.01 |
| Zeta potential (mV) | -0.53 ± 0.09 | -3.51± 0.13 | -3.01± 0.18 | -1.51 ± 0.22 |
| Refractive index | 1.42 ± 0.01 | 1.43 ± 0.03 | 1.42 ± 0.02 | 1.43 ± 0.01 |
| Viscosity (cp) | 44.40 ± 0.82 | 53.61 ± 0.99 | 66.23 ± 1.49 | 47.01 ± 0.45 |
| pH | 6.67 ± 0.31 | 6.72 ± 0.14 | 6.77 ± 0.23 | 6.68 ± 0.20 |
| Thermodynamic stability[(a)] | Stable | Stable | Stable | Stable |
| Physical stability (months) | > 12 | > 12 | > 12 | > 12 |

[(a)] there was no precipitation, phase separation or color changes after the microemulsions (MEs) were subjected to the three stress tests (heating-cooling cycle, centrifugation, and freeze- thaw cycle).

The results of the shear stress and viscosity at different shear rates are shown in Fig. 2. The viscosity of the hydrogels decreases with increasing shear rate. At the initial stage, the viscosity of MEBHG2 was higher than that of MEBHG1, but at the end of the test, both approached zero. The thixotropic behavior of MEBHG1 was slightly higher than that of MEBHG2. The yield stress for MEBHG1 and MEBHG2 were 118.03 ± 6 Pa and 99.56 ± 4 Pa, respectively.

### 2.3. Skin irritation study

The irritation scores (ISs) of different MEs and MEBHGs were determined to evaluate the skin irritation potential of formulations (Table 2) using HET-CAM. The test was conducted according to the principles of Good Laboratory Practices (GLP). Moreover, the controls carried along with the test prove the validity and integrity of the test approach and meet the criteria defined accordingly. The results indicate that all the tested formulations show no evidence for irritation potential. 1% SLS had higher IS values, which is classified as strongly irritant.

**Table 2: Results of cytotoxicity study (mean ± SD, number of tests stated in brackets)**

| Test sample | Irritation score (IS) | Severity | | | Irritation potential as per ICCVAM |
|---|---|---|---|---|---|
| | | H | L | C | |
| Sterile water (n=12) | 0 | 0 | 0 | 0 | No |
| 1% SLS (n=12) | 10.81 | 1.50 ± 0.48 | 0.30 ± 0.65 | 2.80 ± 0.00 | Strong |
| ME1 (n=6) | 0 | 0 | 0 | 0 | No |
| ME2 (n=6) | 0 | 0 | 0 | 0 | No |
| ME3 (n=6) | 0 | 0 | 0 | 0 | No |
| MEBHG1 (n=6) | 0 | 0 | 0 | 0 | No |
| MEBHG2 (n=6) | 0 | 0 | 0 | 0 | No |
| MEBHG3 (n=6) | 0 | 0 | 0 | 0 | No |

### 2.4. Ex vivo permeation study

The degree of permeability of the FAAs from the formulations into the different layers of the pig ear skin was determined after 300 min (Fig. 3). FAAs from ME vehicles show increased permeation as compared to the H-Cream.

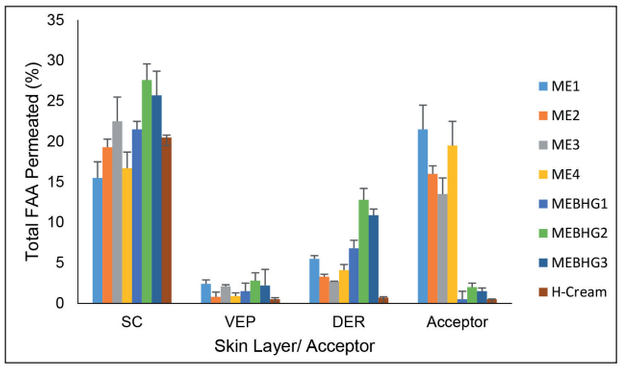


Fig. 3: Percentage of total free amino acids (FAAs) permeated into different layers of the skin from the various formulations (mean ± SD, SC: stratum corneum, VEP: viable epidermis, DER: dermis, ME1 to ME4: microemulsion 1 to 4, MEBHG1 to MEBHG3: microemulsion-based hydrogels 1 to 3, H-Cream: hydrophilic cream).

The different MEs also show slightly different permeation behavior. For example, the flux of ME1 was higher than that of ME3, even though the latter had a higher content of surfactant/co-surfactant. The permeation of the FAAs to the deeper layers of the skin decreases as the viscosity increases (permeation from MEs was much better and deeper than the MEBHGs). Comparing the two polymers, Poloxamer® 407 based MEBHG2 and MEBHG3 permeated to the different layers of the skin as compared to Carbopol® 934 containing MEBHG1.

### 2.5. Assay content

The assay content of the FAAs loaded into the different formulations were investigated using a validated HPLC/DAD analytical method (Kahsay et al. 2022). The assay value for all the formulations is shown in Table 3.

## 3. Discussion

FAAs are assumed to follow the corneocytary pathway (diffusion into the corneocytes) when they are applied to the skin. The delivery of these compounds to the desired site of the skin is challenging due to their hydrophilic nature. In the present study, colloidal preparations (in the form of MEs and MEBHGs) were prepared to overcome the barrier function of the SC. As shown in Table 1, the prepared MEs had small (nano-size internal droplets) and uniform droplet size (PDI close to zero) indicating their desired particle properties (Souto et al. 2022). The small droplet size of the MEs might be due to the lowering of the interfacial tension by the surfactant mixture. The surfactant mixture reduces the curvature of nano-droplets, therefore providing an extremely low globule size (Tenjarla 1999). The particle size of ME3 was highest among all the MEs which could be due to the higher concentration of oil in this formulation. The prepared MEs had low viscosities implying that they can spread easily on the skin. The viscosity increased with increasing surfactant concentration (viscosity of ME1 < ME2 < ME3) and this might be due to the intrinsic viscosity of surfactants (Roohinejad et al. 2015). The refractive index of all the MEs was consistent and was close to that of water (1.33) confirming that the MEs were oil-in-water type. The pH value for all MEs was nearly neutral and this is acceptable for products that are meant for topical application (Martinez-Pla et al. 2004). All MEs were also stable over a period of 12 months indicating the suitability of the formulation design and the selected formulation ingredients.

The low viscosity of MEs is often considered a limitation for application to the skin. To overcome this problem, their viscosity was increased by the addition of polymers (Carbopol® 934 (MEHG1) and Poloxamer® 407 (MEBHG2 and MEBHG3). The rheological properties of these two polymers were compared. MEBHG2 and MEBHG3 had similar rheological properties and hence only MEBHG1 and MEBHG2 were compared. As shown in the frequency sweep experiment (Fig. 1), the storage modulus G' was higher than the loss modulus G'' in both gelling agents. This indicates that the elastic properties prevailed over the viscous behavior and hence structural stability in the tested range. Over the range of angular frequencies from 100 to 0.1 rad/s the G' values showed a weak frequency dependence indicating that both formulations are within the gel state. Comparing the two polymers, those thickened with Poloxamer 407 (MEBHG2) were characterized by enhanced toughness (higher values of G′ modulus)

**Table 3: Assay content of the FAAs in the different formulations (n=3, mean ± SD)**

| FAA | Assay (%) | | | | | |
|---|---|---|---|---|---|---|
| | ME1 | ME2 | ME3 | MEBHG1 | MEBHG2 | MEBHG3 |
| L-Arg | 94.60 ± 1.49 | 92.67 ± 1.04 | 94.73 ± 1.97 | 95.50 ± 1.32 | 94.80 ± 1.93 | 97.20 ± 1.64 |
| L-Asn | 95.52 ± 1.27 | 95.90 ± 1.47 | 95.90 ± 1.92 | 96.33 ± 1.15 | 97.47 ± 1.29 | 95.43 ± 1.25 |
| L-Gln | 96.50 ± 1.32 | 96.40 ±1.64 | 96.60 ± 0.53 | 96.73 ± 1.27 | 95.57 ± 1.69 | 96.20 ± 1.39 |
| L-Ser | 96.73 ± 1.21 | 96.93 ± 1.30 | 96.83 ± 1.61 | 94.40 ± 1.64 | 96.03 ± 1.27 | 97.80 ± 0.92 |
| L-Asp | 94.93 ± 1.90 | 93.73 ± 1.03 | 96.43 ± 1.40 | 97.47 ± 0.50 | 97.47 ± 0.92 | 95.53 ± 0.50 |
| L-Glu | 94.83 ± 2.02 | 97.17 ± 1.66 | 95.60 ± 1.64 | 95.60 ± 1.44 | 96.20 ± 0.72 | 96.20 ± 1.71 |
| L-Thr | 96.13 ± 1.72 | 95.03 ± 1.54 | 95.63 ± 0.64 | 96.27 ± 0.64 | 94.53 ± 1.29 | 96.73 ± 1.62 |
| L-Gly | 96.70 ± 1.70 | 94.33 ± 1.14 | 95.13 ± 1.72 | 96.57 ± 1.40 | 95.30 ± 1.47 | 94.53 ± 1.36 |
| L-Ala | 94.30 ± 1.13 | 93.37 ± 0.64 | 96.13 ± 1.68 | 96.83 ± 1.04 | 96.77 ± 0.97 | 96.77 ± 1.69 |
| L-Pro | 96.47 ± 1.36 | 95.73 ± 1.55 | 96.57 ± 1.34 | 96.33 ± 0.56 | 94.13 ± 1.47 | 96.03 ± 1.75 |
| L-Met | 97.83 ± 1.32 | 94.83 ± 1.04 | 96.17 ± 1.89 | 96.83 ± 1.61 | 97.57 ± 1.44 | 96.47 ± 1.42 |
| L-Val | 93.30 ± 1.54 | 94.67 ± 1.92 | 95.43 ± 1.83 | 97.93 ± 1.10 | 97.03 ± 2.12 | 97.47 ± 1.36 |
| L-Phe | 95.20 ± 1.71 | 94.53 ± 1.75 | 96.70 ± 1.21 | 95.10 ± 1.65 | 95.87 ± 1.21 | 94.37 ± 1.98 |
| L-Ile | 96.67 ± 1.33 | 93.83 ± 1.26 | 99.03 ± 1.70 | 95.60 ± 1.44 | 98.17 ± 0.29 | 95.73 ± 1.62 |
| L-Leu | 92.17 ± 1.04 | 94.60 ± 1.04 | 96.20 ± 0.72 | 95.93 ± 1.01 | 96.87 ± 0.81 | 95.90 ± 1.28 |
| L-lHis | 96.87 ± 1.48 | 93.70 ± 1.81 | 97.37 ± 1.02 | 97.33 ± 1.15 | 96.73 ± 0.64 | 95.13 ± 1.21 |
| L-Orn | 97.23 ± 0.68 | 94.47 ± 1.40 | 94.87 ± 1.03 | 97.63 ± 1.58 | 94.27 ± 1.42 | 95.71 ± 0.61 |
| L-Lys | 95.23 ± 1.08 | 94.57 ± 1.91 | 97.07 ± 1.10 | 97.67 ± 1.15 | 96.83 ±1.61 | 95.81 ± 0.86 |

in the presence of shearing forces than that of Carbopol based hydrogel (MEBHG1). This shows the formation of an extended three-dimensional network and hence strong elastic behavior when Poloxamer 407 was used as gelling agent. The lower G' value of the Carbopol based hydrogel (MEBHG1) might indicate the weak interactions between polymer chains resulting also in a weakening of elastic properties (Froelich et al. 2016). In the hysteresis loop (Fig. 2) the upward ramp shows a higher shear stress reading than the downwards ramp indicating that the sample's behavior is time-dependent under shear load. Furthermore, the viscosity of the hydrogels decreases with increasing shear rate. These indicate that the preparations have non-Newtonian shear-thinning behavior. Thixotropic properties are important for the topical application of pharmaceutical semi-solid formulations (Lee et al. 2009). As shown in Fig. 2, the traces of shear stress for increasing and decreasing shear rate overlap with only minor difference and both formulations have thixotropic behavior. The yield stress values of the prepared hydrogels were within the range of typical semisolid formulations (yield stress value greater than 20 Pa) (Dragicevic-Curic et al. 2009).

The surfactant(s) used in the preparation of MEs could irritate or corrode tissues (Zhong et al. 2009). Moreover, the co-surfactants and oils used might irritate the skin when used at higher concentrations. Therefore, it is recommended to investigate the irritation and corrosive potential of the MEs and MEBHGs. Even though there are some established animal *in vivo* methods designed to conduct skin irritation and toxicity studies (Chen et al. 2007; Gannu et al. 2010), they need exploitation of experimental animals. Since recent years, Hen's egg test chorioallantoic membrane (HET-CAM) test was developed as a sound alternative to the animal *in vivo* tests used to investigate the corrosive potential of pharmaceutical preparations on the skin and mucus membranes (Moniruzzaman et al. 2010; Goebel et al. 2010). Hence, this method was used to evaluate the compatibility of the preparations with the skin. The results clearly showed that all the MEs and MEBHGs were non-irritant with all MEs with an IS value zero (same result as that of sterile water) (Table 2). This shows that neither the surfactants mixture nor the oil phase cause skin irritation and corrosion. This could be due to the smaller amount of these components in the formulations.

As shown in Fig. 3, the FAA loaded formulations have different skin permeability. The MEs show greater permeation than the H-Cream since FAAs did not permeate into the deeper layers of the SC and other skin layers even after 300 min from the hydrophilic cream. This might be due to the small droplet size and large surface area to volume ratio of the ME (Schwarz et al. 1995; Zhou et al., 2009). Similar trends were reported in the literature (Friedman et al. 1995; Schwarz et al. 1995; Otto et al. 2009; Sahle et al. 2013). In addition to droplet size, the thermodynamic activity of the FAAs in the ME can also be modified to favor partitioning into the SC (Kreilgaard 2002). The surfactant and co-surfactant in the MEs may also reduce the diffusional barrier of the SC by acting as penetration enhancers (Rhee et al. 2001). Moreover, the permeation enhancers could contribute to this phenomenon. There were also slight differences between the permeation behavior of the MEs. For example, the flux of ME1 was higher than that of ME3, even though the latter had a higher content of surfactant/co-surfactant. This might be due to the lower droplet size in ME1. It could also be the effect of the water on the ME internal structure, which in turn influences drug delivery to the skin. As water itself is seen as a permeation enhancer for hydrophilic compounds, the permeation of the FAAs could increase due to a hydration effect of the SC if the water content in ME is sufficiently high. Similar trends were reported earlier (Delgado-Charro et al. 1997; Araujo et al. 2010; Zhang and Michniak-Kohn 2011; Cichewicz et al. 2013). The incorporation of the polymers (Carbopol® 934 and Poloxamer 407) significantly controlled the permeation of the FAAs into deeper layers of the skin (Fig. 3). The permeation decreases as the viscosity increases (permeation from MEs was much better and deeper than the MEBHGs ($p < 0.05$). This could be due to slower drug diffusion and partitioning that could occur to a smaller extent in viscous formulations limiting drug transport across the SC. Similar findings were reported for other compounds (Huang et al. 2008; Rozman et al. 2009). Comparing the two polymers, Poloxamer® 407 based MEBHG2 and MEBHG3 permeated to the different layers of the skin as compared to Carbopol® 934 containing MEBHG1. This could be due to the temperature dependent gelling property of Poloxamer® 407. MEBHG2 is liquid at room temperature and some part of the FAAs might permeate before forming the in- situ gel on the skin surface. Finally, as indi-

cated in Table 3, the assay values were within the range of (90-110 %) and fulfill the common pharmacopoeia requirements for drug content. This indicated that the FAAs were uniformly distributed throughout the formulations and their loss was minimum during preparation of MEs and MEBHGs. As seen from the results in section 2, the ME prepared from the standard FAAs (ME1) and that prepared from the mushroom extract (ME4) had similar characteristics. Similarly, MEBHG2 and MEBHG3 had almost similar physico-chemical and permeation properties. This indicates that FAAs extracted from nature-based sources can be used as alternative sources in resource constraint conditions.

In conclusion, the study showed that MEs significantly enhanced the permeability of FAAs into and across the SC ($p < 0.05$). Even though Poloxamer-based MEs had higher viscosity at skin temperature, they permeated into deeper skin layers than Carbopol-based MEs. O/W MEs with smaller droplet sizes permeated more into the deeper skin layers than MEs with larger droplet sizes. As compared to the MEs, penetration from MEBHGs was slower. This indicates that preparation of gels of O/W MEs can be used as a means of directing the MEs to the desired layer within the skin. The HET-CAM result showed that all the formulations did not show signs of irritation or inflammation suggesting that they are safe to be applied on the skin and mucus membrane. The particle and permeation properties of the MEs and MEBHGs prepared from the mushroom extracts were close to that of the formulation prepared using standard FAAs suggesting the possible use of nature-based sources for this purpose. In general, even though further evaluation is needed to elucidate the clinical efficacy of such topical dosage forms, it can be concluded that colloidal carrier systems are effective in the delivery of FAAs to the targeted site of the skin.

## 4. Experimental

### *4.1. Materials*

The L-amino acids (L-Ala, L-Arg, L-Asn, L-Asp, L-Gln, L-Glu, L-Gly, L-His, L-Ile, L-Leu, L-Lys, L-Met, L-Orn, L-Phe, L-Pro, L-Ser, L-Thr, and L-Val) were purchased from Sigma-Aldrich (St. Louis, USA). HPLC grade Fmoc-Cl, L-ornithine monohydrochloride, boric acid, sodium hydroxide, Brij O10, and transcutol P were also obtained from Sigma-Aldrich Chemie GmbH (Steinheim, Germany). Carbopol® 934 was obtained from SERVA Electrophoresis GmbH (Heidelberg, Germany). Isopropyl myristate (IPM) and Poloxamer® P407 was sourced from Caesar and Loretz GmbH (Hilden, Germany). Adamantanamine (ADAM) was sourced from Thermo Fischer Scientific (Heysham, United Kingdom). HPLC grade water and acetonitrile were commercial products of Fischer Chemical (Loughborough, UK). Analytical grade glacial acetic acid and triethyl amine were originated from Carl Roth GmbH + Co. KG (Karlsruhe, Germany). Isopropyl myristate was sourced from Caesar and Loretz GmbH (Hilden, Germany). D-Squame stripping discs were purchased from CuDerm (Dallas, TX, USA). Pig ear was obtained from local pig slaughterhouse in Halle/Saale, Germany. Oyster mushroom was obtained from local supermarkets in Addis Ababa, Ethiopia. The AmberLite™ XAD™16N Polymeric Adsorbent was purchased from Sigma Aldrich, Germany.

### *4.2. Preparation and purification of FAA enriched crude extract*

Among the several plants investigated earlier, oyster mushroom was found to be a viable alternative source of most of the FAAs (Kahsay et al. 2021). Hence, FAAs enriched extract was separated and purified from this fungus as follows. Briefly, the oyster mushrooms were collected from local supermarkets in Addis Ababa. Any dirt on the surface of the samples was manually removed and the samples were gently dried in a drying oven at 40 $^0$C until constant weight. The dried samples were powdered using a mortar and pestle and stored in tightly packed vials until further use. 200 g of the dried samples was mixed with 500 mL of 80% methanol in water and extracted using a magnetic stirring bar at 500 RPM for 6 h. The samples were then sonicated for another hour and filtered through whatman filter number 1 (cellulose filter, pore size 11 µm) (Merck, Germany). The residue from the filtration was further extracted with 400 mL of 80% methanol using sonication (1 h). The filtered extracts from the two extractions were pooled and the methanol was evaporated under reduced pressure at 40 °C. AmberLite™ XAD™16N resin, which was shipped as a water-wet product imbibed with sodium chloride and sodium carbonate salts (to inhibit bacterial growth), was first pre-treated by washing with water followed by regeneration with methanol. The resin was then transferred to a separation column and the concentrated mushroom extracts were separated and purified using this pre-treated resin. The operating conditions were conducted within the recommended operating conditions from the resin manufacturer at room temperature. After conditioning the resin with methanol followed by water (at a rate of 2 bed volume per hour (2 BV/h), 1 BV = 1 $m^3$ solution per $m^3$ resin), the crude extract was loaded to the separation and purification column containing the pre-treated AmberLite™ XAD™16N resin (at sample loading rate of 2 BV/h). Then the FAAs were eluted using 80% methanol at an elution rate of 2 BV/h. The fractions which gave positive response to the ninhydrin test were pooled. The methanol was evaporated under reduced pressure at 40 °C. Finally, the water extract was freeze dried (Alpha 2–4-LSC, Martin Christ Gefriertrocknungsanlagen GmbH, Germany), transferred to a glass vial and stored at -4 $^0$C until further study. The extract contained 18 FAAs (L-Ala, L-Arg, L-Asn, L-Asp, L-Gln, L-Glu, L-Gly, L-His, L-Ile, L-Leu, L-Lys, L-Met, L-Orn, L-Phe, L-Pro, L-Ser, L-Thr, and L-Val).

### *4.3. Selection of formulation ingredients*

*Surfactant*: Among others, Brij® O10, a Polyoxyethylene (10) oleyl ether, was selected as surfactant. It has a single polar long POE chain linked to the oleyl group through polyhydric sorbitan and this can promote the permeation of the FAAs to the desired site. Increasing water content in Brij® O10-based MEs increased the ME existence area. Brij® O10 hydrophilic chains are strongly hydrated and connected with hydrogen bonds, allowing the interaction with more water droplets (Podlogar et al. 2004). Due to these properties, this surfactant can be used in aqueous emulsions to assist in the (trans)dermal delivery of drugs.

*Co-surfactant*: Transcutol® P is non-irritant, an effective solubilizer and skin penetration enhancer. It has been used for decades in dermal applications without adverse effects being reported (Osborne 2011). In our study on the effect of different diffusion enhancers on the corneocyte-water partitioning properties of the FAAs (results not included), it was found that Transcutol® P has the highest positive effect among the tested corneocyte diffusion enhancers. Hence, due to its unique properties, it was selected as co-surfactant in preparing the MEs.

*Permeation/diffusion enhancer*: To deliver the required quantity of FAAs, DMSO was used as additional diffusion enhancer. It is one of the first and intensively studied hydrophilic penetration/diffusion enhancers. It does not disrupt the lipid layer of the SC if used in pharmaceutically and cosmetically relevant concentrations (less than 30%). Hence, the permeation/diffusion enhancing effect of DMSO for the topical application of hydrophilic drugs appears to be realized via the corneocytes (Mueller et al. 2019).

*Oil phase*: Isopropyl myristate (IPM) was selected as an oil phase as its usage in the (trans)dermal system has add-on benefit being a biocompatible permeation enhancer (Kantaria et al. 2003; Zidan et al. 2017; Furuishi et al. 2019). Considering the above-mentioned specifics, we conjectured that the encapsulation of FAAs in Brij® O10 /Transcutol/ IPM/ water/ DMSO in the form of MEs may result in enhanced permeation of FAAs across the epidermal barrier and can achieve greater dermal bioavailability. It is well documented that O/W MEs have improved permeation as compared to bicontinuous MEs and W/O MEs (Araujo et al. 2010; Cichewicz et al. 2013). Hence, the MEs were prepared in an O/W ME type.

*Gelling agents*: The low viscosity of MEs is often considered a limitation for application to the skin. To overcome this problem, their viscosity has been increased with the addition of two polymers (Carbopol® 934 and Poloxamer® 407).

*Active ingredient*: The MEs and MEBHGs were prepared using both the standard FAAs containing these FAAs and the FAA enriched extracts. The extract and the FAAs standard mixture contains 18 FAAs (L-Ala, L-Arg, L-Asn, L-Asp, L-Gln, L-Glu, L-Gly, L-His, L-Ile, L-Leu, L-Lys, L-Met, L-Orn, L-Phe, L-Pro, L-Ser, L-Thr, and L-Val).

**Table 4: Composition of different microemulsions (MEs) and microemulsion-based hydrogels (MEBHGs) loaded with free amino acids**

| S/N | Ingredients | Formulation composition (% W/W) | | | | | | |
|---|---|---|---|---|---|---|---|---|
| | | ME1 | ME2 | ME3 | ME4 | MEBHG1 | MEBHG2 | MEBHG3 |
| 1 | Free amino acid standard mixture* | 0.5 | 0.5 | 0.5 | - | 0.5 | 0.5 | - |
| 2 | Free amino acid mushroom extract** | - | - | - | 0.5 | - | - | 0:5 |
| 3 | Brij® O10: Transcutol® P (1:1) | 26 | 32 | 38 | 26 | 26 | 26 | 26 |
| 4 | Isopropyl myristate | 4 | 8 | 12 | 4 | 4 | 4 | 4 |
| 5 | Water: DMSO (9:1) | 70 | 60 | 50 | 70 | 70 | 70 | 70 |
| 6 | Carbopol ® 934 | - | - | - | - | 1 | - | - |
| 7 | Poloxamer 407 | - | - | - | - | - | 16 | 16 |
| 8 | 2-phenoxyethanol | - | - | - | - | 1 | 1 | 1 |

*The free amino acid standard mixture contains 18 FAAs (L-Ala, L-Arg, L-Asn, L-Asp, L-Gln, L-Glu, L-Gly, L-His, L-Ile, L-Leu, L-Lys, L-Met, L-Orn, L-Phe, L-Pro, L-Ser, L-Thr, and L-Val). **The mushroom extract contains all the stated free amino acids.

### 4.4. Preparation of MEs and MEBHGs

Oil-in-water MEs loaded with FAAs were prepared by mixing all the components of the ME (Table 4). Oil, surfactant/co-surfactant mixture and hydrophilic phase containing the FAAs were mixed in a glass vial until a clear and homophasic ME was formed. The MEs which contain 18 FAAs were prepared using both the standard FAAs (ME1-ME3) and the FAA enriched crude extracts obtained from oyster mushroom (ME4). The prepared MEs were stored in glass vials at room temperature. MEBHGs were prepared using two different gelling agents (Carbopol® 934 and Poloxamer® 407). Carbopol® 934 based hydrogels were prepared by incorporating Carbopol® 934 to ME1. Then a few drops of triethanolamine was added to make the gels. Poloxamer® 407 gels were prepared by the cold method. In that process, the two MEs (ME1 and ME4) were first cooled to 4 °C and then the required amount of Poloxamer® 407 was added slowly with continuous mixing to each of the MEs while the temperature was kept at 4 °C. The final hydrogel was mixed and stored at 4 °C until a clear hydrogel was formed. A few drops of 2-phenoxyethanol were added to both hydrogels as stabilizer (1% of the total ME gel). The MEBHGs were stored in glass vials protected from light.

### 4.5. Preparation of FAA loaded non-ionic hydrophilic cream.

FAA mixture (5 mg) was incorporated into 1 g of non-ionic hydrophilic cream (DAC). The cream is composed of non-ionic emulsifying alcohol (21%), 2-ethylhexyl laureate (10%), glycerol (85%) (4.5%), potassium sorbate (0.14%), anhydrous citric acid (0.07%), and double distilled water (63.79%).

### 4.6. Characterization of MEs and MEBHGs

The physical stability of the MEs was routinely evaluated at ambient conditions by visual inspection of the samples over a period of time (until 12 months). Any physical change, such as phase separation, turbidity, flocculation of the droplets and/or precipitation of dispersed lipids, was taken as indicators of instability. The isotropicity of the formulation was verified using a cross-polarised light microscope (Zeiss Axiolab Pol, Carl Zeiss MicroImaging GmbH, Jena, Germany) where a clear system that appears as dark background was categorized as ME.

The refractive index of stable MEs was obtained using an Abbe refractometer (Carl-Zeiss, Jena, Germany) at 25±2 °C. The viscosity of the MEs was measured at 25±0.2 °C using a rotational viscometer (Anton Paar GmbH, Graz, Austria). The pH values of the samples were evaluated using digital pH meter (S20-K, Mettler Toledo, Switzerland). Readings were made in triplicate and the average, and the RSD was calculated. The particle sizes and zeta potentials were determined with the Malvern Instruments Zetasizer Nano ZS by Malvern Panalytical GmbH (Kassel, Germany). For particle size measurements, samples were diluted at 1:10 in water and measured in triplicate with 15 runs each at 25 °C in back scattering mode. The average results and the polydispersibility index (PDI) were calculated. The zeta potential was determined in triplicate by diluting each sample 1:1 in 0.1 x PBS with pH 7.4 at 25 °C with 50 runs per measurement.

Rheological measurements of the gel formulations were conducted at 32 °C by a rotational viscometer equipped with a cone-and-plate geometry of 25 mm diameter (the cone angle was 1°). All the formulations were subjected to frequency sweep measurements at a fixed deformation amplitude in the LVR (below the critical strain level) by varying the angular frequency (100 to 0.1 rad/s). The storage modulus (G') represents the elastic portion of the viscoelastic behavior, which quasi describes the solid-state behavior of the hydrogel and the loss modulus (G'') characterizes the viscous portion of the viscoelastic behavior, which can be seen as the liquid-state behavior of the sample were evaluated and compared. Steady shear measurements with increasing and decreasing shear rates (hysteresis loops) were also made for each gel formulation. Each measurement consisted of three parts: a stepwise increase in shear rate from 1 $s^{-1}$ to 100 $s^{-1}$ with 21 measurement points, 10 measurement points with a constant shear rate of 100 $s^{-1}$ for 5 seconds each, and finally, a stepwise decrease in shear rate from 100 $s^{-1}$ to 1 $s^{-1}$ with 21 points (with 5 s measurement time for each rate). The yield stress and thixotropic behaviour of the gels were evaluated.

The thermodynamic stability of MEs was assessed by the three-step procedure (heating-cooling cycle, centrifugation test and the freeze-thaw cycle) as reported by Shafiq et al. (2007). In the heating-cooling cycle, the MEs underwent 6 cycles, where they were kept at 40±2 °C and then at 4±2 °C for at least 48 hours. For the centrifugation test, the MEs underwent centrifugation at 3,500 rpm for 30 min and were scrutinized for any drug precipitation or phase separation or any color/consistency changes. Finally, for the freeze-thaw cycles, the formulations were stored between −25±2 °C and 25±2 °C at least for 48 h. After each test, the MEs were examined for any drug precipitation or phase separation or any color/consistency changes.

### 4.7. Hen's egg test chorioallantoic membrane (HET-CAM)

An *ex vivo* toxicity study of the MEs was carried out as per the HET-CAM (Sahle et al. 2014). Naturally fertilized chicken eggs (50-60) g of the New Hampshire breed being provided on the day of the laying by the Livestock Research Center of the Martin Luther University of Halle-Wittenberg were used. After transport in polystyrene-coated containers, the eggs were incubated in pallets in an incubator for 8 days at 37 °C and 55% air humidity. Every 12 h, the eggs were turned, except for the last 24 h (9th day of incubation). After the end of the breeding phase (10th day of incubation) the eggs were transferred individually into polystyrene coatings, opened and prepared micro surgically at room temperature as described below.

After candling the egg poles with a high-intensity cold light source, a circular hole with a diameter of 1,5 cm was cut near the air chamber into the weaker convex pole of the eggs. The dust caused during the opening was carefully blown off the amnion without any contact using a rubber bellows, and the amnion was wetted with 37 °C warm saline (0,9% NaCl). After careful dissection with microsurgical cutlery 20-30 min after the opening of the eggs and a resting phase in the incubator, the outer egg membrane was removed under a laminar flow hood and the CAM was exposed. Approximately 10-30 % of the prepared eggs were not fertilized and had to be discarded. Only eggs were used for the tests, which had a well-developed vascular network on the CAM. For applications, 300 µL of each ME was administered to 6 eggs in each case not later than 30 min after preparation of eggs. Sterile water (negative control) and 1% sodium lauryl sulphate (SLS) (positive control) were applied on the CAM as reference solutions. In the collection of the scores, first, an observation of the eggs within a total period of 5 minutes (300 seconds) was conducted. During this period, changes in the CAM according to the following criteria regarding the time of occurrences (irritation score, IS) and their severity at the end of the observation period were documented. Occurrences of bleeding (hemorrhage), i.e., the extravasation of erythrocytes was classified as hemorrhage (H). Vessels being lysed or becoming transparent were classified as lysis of vessels (L). Stagnation of blood flow and signs of intravascular coagulation were classified as coagulation (C).

The calculation of the irritation score (IS) was performed according to the CICCVAM criteria using the following procedure (ICCVAM 2006):

$$IS = \left(\frac{301 - secH}{300} x\ 5\right) + \left(\left(\frac{301 - secL}{300}\ x\ 7\right)\right) + \left(\frac{301 - secC}{300}\ x\ 9\right)$$

where, IS = Irritation score, sec= seconds until the on-set of the effect, H= hemorrhage, L = Lysis and, C= Coagulation.

The following threshold values were defined for the evaluation criteria: IS ≤ 1= no evidence of irritation potential, IS > 1 and ≤ 4= slight irritation potential, IS > 4 and ≤ 9 = moderate irritation potential and IS > 9 = strong irritation potential. The severity of changes versus the end of the observation period was evaluated using the following criteria: 0= no response, 1= mild reaction, 2= moderate reaction, and 3= strong reaction. The hemorrhage (H) was assigned semi-quantitatively, according to the degree of erythrocyte extravasates, to the following categories: Single capillary bleedings in morphologically intact capillaries were classified as mild, multiple capillary bleedings in morphologically intact capillaries as moderate, and morphologically damaged capillaries with capillary bleedings or mass bleedings as heavy H. Scattered transparent capillary sections were evaluated as light, transparency of all capillaries as moderate and the incidence of complete lysis of vessels as heavy L. Coagulation (C) was assigned semi-quantitatively, according to the degree of coagulation phenomena, to the following categories: Single capillary thrombosis in morphologically intact capillaries were classified as mild, multiple capillary thrombosis in morphologically intact capillaries as moderate, and damaged capillaries with extended segments of capillary thrombosis as heavy C. After the end of the experiments, all eggs were killed during 48 hours in the freezer at -20 °C and then disposed hygienically in the hospital waste.

### 4.8. Ex vivo permeability study

Pig ears obtained from a local slaughterhouse in Halle (Saale), Germany were used for the *ex vivo* permeation study (Salerno et al. 2015). The pig ears were carefully cleaned with water. The hair from the outer region of the ears was removed and then the skin was carefully separated from cartilage using a scalpel. Subsequently, adipose subcutaneous tissue was removed. Circular pieces of skin (19 mm in diameter, 1.6±2 mm in thickness) were punched from the best areas of the separated skin, hermetically sealed in tinfoil, packed in an occlusive polyethylene bag, and stored at –20 °C. Just before the experiment began, skin samples were defrosted at room temperature and the surface was dried using cotton pads, and dermatomed to nominal thickness (ca. ≥ 1 mm), using the manual dermatome or scalpel blades (OECD 2004). The experimentally obtained thickness was determined using a digital caliper. All prepared skin samples were punched to 19 mm disks. The outer border of the application area of the excised pig was marked. It was then mounted on unjacketed vertical Franz diffusion cells (Franz and Barker 1977) (with 3 ml of acceptor volume, 9 mm orifice internal diameter (orifice area of 0.64 $cm^2$), and a 5 mL receptor volume) (SES GmbH Analysesysteme, Bechenheim, Germany). The receptor compartment was filled with phosphate-buffered saline pH 7.4 and was continuously stirred at 600 RPM throughout the experiment. The temperature of the cell was maintained at 32 °C using an incubator.

The skin mounted in the cell was allowed to rest for an hour in contact with receptor media before the application of the samples. Twenty milligram (20 mg) of each formulation was applied onto the epidermal skin side and evenly distributed within the application area (0.64 $cm^2$) and was allowed to permeate for 300 min. A mass balance study was conducted after the 300 min permeation period. The apparatus was disassembled, the remaining formulation on the skin surface was thoroughly wiped with a cotton swab and transferred to a 2mL Eppendorf tube. One milliliter (1 mL) of methanol was added and the FAAs were extracted; resulting solutions were sonicated for 10 min, centrifuged at 5000 g for 10 min (Centrifuge Mega Star 3.0R, VWR International, LLC, Darmstadt, Germany). The supernatant was transferred to another 2 mL Eppendorf tube and concentrated under vacuum in an Eppendorf Concentrator (Model 5301, Eppendorf, Hamburg, Germany) at 45 °C for 45 min. This sample was labeled "swab". After removing the remaining formulation on the surface, the SC was removed by employing the tape stripping method (D-Squame Stripping Discs (CuDerm (Dallas, TX, USA)). Application of the adhesive tape was followed by uniform pressure for a fixed time (225 g/$cm^2$, 10 s) (Sølberg et al. 2019). The strips were then removed with a tweezer in a quick uniform movement, following the longitudinal axis of the skin sample. SC was sequentially removed using 30 consecutive strips (Sølberg et al. 2019) applied on the same skin area with a new tape being used for each application. Then the strips were pooled into six 2mL Eppendorf tubes (each containing 5 strips) and each was extracted with 500 µL methanol. The solutions were concentrated under vacuum in an Eppendorf Concentrator (Model 5301, Eppendorf, Hamburg, Germany) at 45 °C for 30 min and the resulting solutions were further pooled to two 2 mL Eppendorf tubes. The pooled samples were further concentrated under vacuum in an Eppendorf Concentrator at 45 °C for 45 min. The

resulting solutions were labeled as $SC_1$ and $SC_2$. The excess skin around the diffusion area was removed and the viable epidermis was separated from the dermis using a heat method (Zou et al. 2017). For this, the skin was sandwiched in aluminum foil and pressed on a slide warmer at 50 °C for 50 s. Then the viable epidermis layer was gently peeled from the dermis with dissection forceps, cut into small pieces, and transferred to a 2 mL Eppendorf tube. This sample was labeled VEP. The remaining dermal part was cut (longitudinal axis) into five equal small pieces with a thickness of about 200 µm and these were labeled DER1-DER5 from the epidermis side to the lower parts of the dermis. The skin pieces were quantitatively transferred to different 2 mL Eppendorf tubes. Five hundred microliter (500 µL) of methanol was added to each sample containing the VEP and DER1-DER5 and the skin samples were mixed thoroughly for 20 min on a vortex (JK Janke and Kunkel IKA, model IKA VIBRAX-VXR). Then a steel ball of 5 mm in diameter was inserted to each of the Eppendorf tubes and the skin samples were homogenized using a mixer mill (Model MM 301, Retsch GmbH, Germany) at 25 cycle per second for 5 min. The homogenized skin samples were centrifuged at 5000 g for 10 min. The supernatants were concentrated under vacuum in the Eppendorf Concentrator at 45 °C for 45 min. Finally, 200 uL of the receptor medium was transferred to 1.5 mL Eppendorf tube, centrifuged at 5000 xg for 10 min, and the supernatant was transferred to another 1.5 mL Eppendorf tube, and this was labelled as "receptor". The FAA content in each of the samples taken from the acceptor liquid, surface of the skin, tape stripping and the skin samples were analyzed using an HPLC/DAD method. Each of the concentrated solutions (swab, SC1, SC2, EP+DER1, DER2, DER3, DER4, and DER5) were reconstituted with 100 µL water. Then each solution (including the permeated part) was derivatized as per the procedure stated in section 2.3 (starting from the addition of 200 µL of 0.5 M sodium borate buffer pH 8.6) and analyzed using the HPLC/DAD method (Kahsay et al. 2022).

### *4.9. Assay content of the FAAs in the formulations*

#### *4.9.1. Preparation of standard solutions*

Twenty milimolar (20 mM) stock solutions of each of the selected FAAs were prepared in 2-mL Eppendorf tubes using water as solvent. Then, 50 µL of each stock solution was transferred to a 1.5-mL Eppendorf tube and diluted to 1,000 µL with the same solvent to obtain a stock solution of 1 mM. A series of six standard solutions having a concentration of 50, 100, 200, 400, 600, and 800 µM were then prepared by transferring appropriate volumes of the stock solution and diluting with water in separate 1.5 µL Eppendorf tubes.

#### *4.9.2. Preparation of samples*

A stock solution of the formulation containing about 2.5 mg/mL of the respective FAA was extracted using methanol as solvent. The resulting solutions were then filtered through Whatman filter paper No. 42 and 40 µL of the filtrate were further diluted to 200 µL with bidistilled water.

#### *4.9.3. Derivatization*

One hundred microliter (100 µL) of each of the standard and sample solutions were transferred to 1.5 mL Eppendorf tubes. Two hundred microliters (200 µL) of 0.5 M sodium borate buffer pH 8.6 and 400 µL 6 mM Fmoc-Cl solution (in acetonitrile) were added to each solution. The resulting solutions were mixed very well and incubated for 10 min for complete derivatization. Three hundred microliters (300 µL) of 12.5 mM Adamantane HCl (in water: acetonitrile, 1:3 v/v) were added to each solution to terminate the reaction. The solutions were mixed again and incubated for another 2 min. Then each solution was centrifuged (Model Mega Star 3.0R, VWR International, LLC, Darmstadt, Germany) at 10,000 g for 5 min, and the supernatant was transferred to an HPLC autosampler vial.

#### *4.9.4. HPLC chromatographic conditions*

The chromatographic apparatus consisted of Shimadzu HPLC system (Shimadzu Corporation, Tokyo, Japan) with Solvent Delivery Module LC-40D, Auto-sampler Module SIL-40C, Diode Array Detector Module SPD-40M, Column Oven Module CTO-40C, and System Controller Module CBM-40. Chromatographic separations were conducted on InfinityLab Poroshell 120 E.C 18 (3 x 50) mm, with particle size of 2.7 µm (Agilent Technologies Germany GmbH & Co. KG, Waldbronn, Germany). Solvent A and solvent B consisted of water and acetonitrile, respectively, and each contained 0.2% glacial acetic acid and 0.1% trimethylamine as pH adjusters. The gradient system was adjusted as follows (time (min), %B): 0/15, 4/15, 7/24, 16/24, 18/45, 21/45, 24/70, 25/15. The auto-sampler temperature was maintained at 4 °C; 10 µL of each sample were injected. The column temperature was maintained at 25 °C and the detection of the derivatized samples was performed using diode array detection. The total run time was set at 26 min.

#### *4.9.5. Calculation*

The peak area of the standard and sample solutions were recorded and the concentration of each FAA in the different fractions was calculated from the slope and regression line of the respective calibration curves obtained from the standard solutions.

Acknowledgments: The authors would like to thank Johannes Gutenberg-University, Mainz, Germany and Martin Luther University Halle-Wittenberg, Germany for providing the necessary materials and the laboratory facility to conduct this research.

Conflict of interest statement: The authors declare no conflict of interest.

## References

Alkrad JA, Al-doori SM, AlGhatm H (2019) Using inverted micro emulsions for transdermal application of folic acid. Asian J Pharm Sci 13: 134–40.

Araujo L.M, Thomazine JA, Lopez RF (2010) Development of micro emulsions to topically deliver 5-aminolevulinic acid in photodynamic therapy. Eur J Pharm Biopharm 75: 48–55.

Arezki NR, Williams AC, Cobb JA, Brown MB (2017) Design, synthesis, and characterization of linear unnatural amino acids for skin moisturization. Int J Cosmet Sci 39: 72–82.

Azeem A, Khan ZI, Aqil M, Ahmad FJ, Khar RK, Talegaonkar S (2009) Microemulsions as a surrogate carrier for dermal drug delivery. Drug Devel Ind Pharm 35: 525–547.

Biruss B, Valenta C (208) The advantage of polymer addition to a non-ionic oil in water micro-emulsion for the dermal delivery of progesterone. Int. J. Pharm 349: 269–273.

Boonme P (2007) Application of micro-emulsions in cosmetics. J Cosmet Dermatol 6: 223–228.

Bouwstra JA, Honeywell-Nguyen PL, Gooris GS, Ponec M (2003) Structure of the skin barrier and its modulation by vesicular formulations. Prog Lipid Res 42: 1–36.

Brown MB, Martin GP, Jones SA, Akomeah FK (2006) Dermal and transdermal drug delivery systems: current and future prospects. Drug Deliv 13: 175–187.

Chen H, Mou D, Du X, Chang D, Zhu J, Liu H, Xu X, Yang (2007) Hydrogel thickened micro emulsion for topical administration of drug molecule at an extremely low concentration. Int J Pharm 341: 78–84.

Cichewicz A, Pacleb C, Connors A, Hass MA, Lopes LB (2013) Cutaneous delivery of α-tocopherol and lipoic acid using micro emulsions: Influence of composition and charge. J Pharm Pharmacol 65: 817–826.

Danielsson I, Lindman B (1981) The definition of micro emulsion. Colloid Surface 3: 391–392.

Delgado-Charro MB, Iglesias-Vilas G, Blanco-Mendez J, Lopez-Quintela MA, Marty JP, Guy RH (1997) Delivery of a hydrophobic solute through the skin from novel micro emulsion systems. Eur J Pharm Biopharm 43: 37–42.

Derakhshandeh K, Erfan M, Dedashzadeh S (2007) Encapsulation of 9-nitrocamptothecin, a novel anticancer drug, in biodegradable nanoparticles: Factorial design, characterization and release kinetics. Eur J Pharm Biopharm 66: 34–41

Dragicevic-Curic N, Winter S, Stupar M, Milic J, Krajisnik D, Gitter B, Fahr A (2009) Temoporfin-loaded liposomal gels: viscoelastic properties and in vitro skin penetration. Int J Pharm 373: 77–84.

El-Laithy HM, El-Shaboury KMF (2002) The development of cutina lipogels and gel micro emulsion for topical administration of fluconazole, AAPS PharmSciTech 3: 35.

Fanun M (2009) Oil type effect on diclofenac solubilization in mixed-nonionic surfactants micro emulsions. Colloid Surface A 343: 75–82

Fowler J (2012) Understanding the role of NMF in skin hydration. Pract Dermatol July 2012: 36–40.

Franz TJ, Barker EA (1977) Finite dose technique as a valid in vitro model for study of percutaneous absorption in man. Clin Res 25: A198.

Friedman D, Schwarz JS, Weisspapir M (1995) Submicron emulsion vehicle for enhanced transdermal delivery of steroidal and nonsteroidal antiinflammatory drugs. J Pharm Sci 84: 324–329.

Froelich A, Osmałek T, Kunstman P, Roszak R, Białas W (2016) Rheological and textural properties of microemulsion-based polymer gels with indomethacin. Drug Dev Ind Pharm 42: 854–861.

Furuishi T, Kunimasu K, Fukushima K, Ogino T, Okamato K, Yonemochi E, Tomono K, Suzuki T (2019) Formulation design and evaluation of a transdermal drug delivery system containing a novel eptazocine salt with the Eudragit® E adhesive. J Drug Deliv Sci Technol 54: 101289.

Gannu RCR, Palem VV, Yamsani SK, Yamsani MR, Yamsani (2010) Enhanced bioavailability of lacidipine via micro emulsion based transdermal gels: formulation optimization, ex vivo and in vivo characterization, Int J Pharm 388: 231–241.

Goebel A, Neubert RHH (2008) Dermal peptide delivery using colloidal carrier systems. Skin Pharmacol. Physiol 21: 3–9.

Goebel AS, Knie U, Abels C, Wohlrab J, Neubert RH (2010) Dermal targeting using colloidal carrier systems with linoleic acid. Eur J Pharm Biopharm 75: 162–172.

Goebel ASB, Schmaus G, Neubert RHH, Wohlrab J (2012) Dermal peptide delivery using enhancer molecules and colloidal carrier systems. Part I: Carnosine. Skin Pharmacol Physiol 25: 281–287.

Groen D, Gooris GS, Barlow DJ, Lawrence MJ, van Mechelen JB, Demé B, Bouwstra JA (2011) Disposition of ceramide in model lipid membranes determined by neutron diffraction. Biophys. J 100: 1481–1489.

Hashem FM, Shaker DS, Ghorab MK, Nasr M, Ismail A (2011) Formulation, characterization and clinical evaluation of micro emulsion containing clotrimazole for topical delivery. AAPS PharmSciTech 12: 879–86

Hua L, Weisan P, Jiayu L, Ying Z (2004) Preparation, evaluation, and NMR characterization of vinpocetine micro emulsion for transdermal delivery. Drug Dev Ind Pharm 30: 657–666.

Huang YB, Lin YH, Lu TM, Wang RJ, Tsai YH, Wu PC (2008) Transdermal delivery of capsaicin derivative-sodium nonivamide acetate using micro emulsions as vehicles. Int J Pharm 349: 206–211

Hussain H, Ziegler J, Hause G, Wohlrab J, Neubert RHH (2019a) Quantitative analysis of free amino acids and urea derived from isolated corneocytes of healthy young, healthy aged, and diseased skin. Skin Pharmacol Physiol 32: 94–100.

Hussain H, Ziegler J, Mrestani Y, Neubert RHH (2019b) Studies of the conreocytary pathway across the stratum corneum. Part I: Diffusion of amino acids into the isolated corneocytes. Pharmazie 74: 340–344.

ICCVAM-Test (2006) ICCVAM Recommended Protocol for Future Studies Using the Hen's Egg Test-Chorioallantoic Membrane (HET-CAM) Test Method.

Izquierdo P, Wiechers JW, Escribano E, Garcia-Celma MJ, Tadros TF, Esquena J, Dederen JC, Solans C (2007) A study on the influence of emulsion droplet size on the skin penetration of tetracaine. Skin Pharmacol Physiol 20: 263–270.

Kahsay BN, Moeller L, Imming P, Neubert RHH, Gebre-Mariam T (2022) Development and validation of a simple, selective, and accurate reversed-phase liquid chromatographic method with diode array detection (RP-HPLC/DAD) for the simultaneous analysis of 18 free amino acids in topical formulations. Chromatographia 85: 665–676.

Kahsay BN, Ziegler J, Imming P, Gebre-Mariam T, Neubert RHH, Moeller L (2021) Free amino acid contents of selected Ethiopian plant and fungi species: a search for alternative natural free amino acid sources for cosmeceutical applications. Amino Acids 53: 1105–1122.

Kantaria S, Rees GD, Lawrence MJ (2003 Formulation of electrically conducting microemulsion-based Organogels. Int J Pharm 250: 65–83

Kaur A, Sharma G, Gupta V, Ratho RK, Katare OP (2018) Enhanced acyclovir delivery using w/o type micro emulsion: preclinical assessment of antiviral activity using a murine model of zosteriform cutaneous HSV-1 infection. Artif Cells Nanomed Biotechnol 46: 346–354.

Kiselev MA, Ryabova NY, Balagurov AM, Dante S, Hauss T, Zbytovska J, Wartewig S, Neubert RH (2005) New insights into the structure and hydration of a stratum corneum lipid model membrane by neutron diffraction. Eur. Biophys. J 34: 1030–1040.

Kogan A, Garti N (2006) Microemulsions as transdermal drug delivery vehicles. Adv Colloid Interface Sci 123–126, 369–385.

Kreilgaard M (2002) Influence of microemulsions on cutaneous drug delivery. Adv Drug Deliv Rev 54: S77-98.

Kumbhar MD, Karpe MS, Kadam VJ (2020) Development and characterization of water-in-oil micro emulsion for transdermal delivery of Eperisone hydrochloride. Appl Clin Res Clin Trials Regul Aff 7(1): 45–64.

Lee CH, Moturi V, Lee Y (2009) Thixotropic property in pharmaceutical formulations. J Control Release 136: 88–98.

Liu CH, Chang FY, Hung DK (2011) Terpene micro emulsions for transdermal curcumin delivery: effects of terpenes and cosurfactants. Colloids Surf B Biointerfaces 82: 63–70.

Martinez-Pla JJ, Martin-Biosca Y, Sagrado S, Villanueva-Camanas RM, Medina-Hernandez MJ (2004) Evaluation of the pH effect of formulations on the skin permeability of drugs by biopartitioning micellar chromatography. J Chromatogr A 1047: 255–262.

Moniruzzaman M, Tamura M, Tahara Y, Kamiya N, Goto M (2010) Ionic liquid-inoil micro emulsion as a potential carrier of sparingly soluble drug: characterization and cytotoxicity evaluation. Int J Pharm 400: 243– 250.

Mueller J, Trapp M, Neubert RHH (2019) The effect of hydrophilic penetration/diffusion enhancer on stratum corneum lipid models: Part II: DMSO. Chem Phys Lipids 104816: 1-8.

Nastiti C, Ponto T, Abd E, Grice JE, Benson HAE, Roberts MS (2017) Topical nano and micro emulsions for skin delivery. Pharmaceutics 9: 37–62

Neubert RHH, Sommer E, Schölzel M, Tuchscherer B, Mrestani Y, Wohlrab J (2018) Dermal peptide delivery using enhancer moleculs and colloidal carrier systems. Part II: Tetrapeptide PKEK. Eur J Pharm Biopharm 124: 28–33.

OECD (2004) Skin Absorption: In Vivo Method. Test Guideline No. 427; Series on Testing and Assessment. No. 428; OECD: Paris, France

Osborne DW, Musakhanian J (2018) Skin penetration and permeation properties of Transcutol®—Neat or diluted mixtures. AAPS PharmSciTech 19: 3512–3533.

Otto A, Plessis J, Wiechers JW (2009) Formulation effects of topical emulsions on transdermal and dermal delivery. Int J Cosmet. Sci 31: 1–19.

Panseria B, Desai K, Vijayendra Swamy SM (2014) Formulation, development, and evaluation of micro emulsion-based hydrogel of econazole nitrate. Pharma Science Monitor 5:86–107.

Park ES, Chang SY, Hahn M, Chi SC (2000) Enhancing effect of polyoxyethylene alkyl ethers on the skin permeation of ibuprofen. Int J Pharm 209: 109–119.

Patil S, Sandberg A, Heckert E, Self W, Seal S (2007) Protein adsorption and cellular uptake of cerium oxide nanoparticles as a function of zeta potential. Biomaterials 28: 4600–4607

Peira E, Scolari P, Gasco MR (2001) Transdermal permeation of apomorphine through hairless mouse skin from micro emulsions. Int J Pharm 226: 47–51.

Podlogar F, Gasperlin M, Tomsic M, Jamnik A, Rogac MB. (2004) Structural characterisation of water-Tween 40/Imwitor 308-isopropyl myristate micro emulsions using different experimental methods. Int J Pharm 276: 115–128.

Rhee YS, Choi JG, Park ES, Chi SC (2001) Transdermal delivery of ketoprofen using micro emulsions, Int. J. Pharm 228: 161.

Roohinejad S, Oey I, Wen J, Lee SJ, Everett DW, Burritt DJ (2015) Formulation of oil-in-water β-carotene microemulsions: effect of oil type and fatty acid chain length. Food Chem 174: 270–278.

Rozman B, Gasperlin M, Tinois-Tessoneaud E, Pirot F, Falson F (2009) Simultaneous absorption of vitamins C and E from topical micro emulsions using recon- structed human epidermis as a skin model, Eur J Pharm Biopharm 72: 69.

Rozman B, Zvonar A, Falson F, Gasperlin M (2009) Temperature-sensitive micro emulsion gel: An effective topical delivery system for simultaneous delivery of vitamins C and E. AAPS PharmSciTech 10: 54–61.

Sahle F, Wohlrab J, Neubert RHH (2014). Controlled penetration of ceramides into and across the stratum corneum using various types of microemulsions and formulation associated toxicity studies. Eur J Pharm Biopharm 86: 244–250.

Sahle FF, Metz H, Wohlrab J, Neubert RHH (2012) Polyglycerol fatty acid ester surfactant-based micro emulsions for targeted delivery of ceramide AP into the stratum corneum: formulation, characterisation, *in vitro* release, and penetration investigation. Eur J Pharm Biopharm 82: 139-150.

Sahle FF, Metz H, Wohlrab J, Neubert RHH (2013) Lecithin-based micro emulsions for targeted delivery of ceramide AP into the stratum corneum: formulation, characterizations, and in vitro release and penetration studies. Pharm Res 30: 538–551.

Salerno C, Gorzalczany S, Arechavala A, Scioscia SL., Carlucci AM, Bregni C (2015) Novel gel-like micro emulsion for topical delivery of Amphotericin B. Rev Colomb Cienc Quím Farm 44: 359–381.

Sapra B, Thatai P, Bhandari S, Sood J, Jindal M, Tiwary AK (2014) A critical appraisal of micro emulsions for drug delivery: part II. Ther Deliv 5: 83–94.

Schroeter A, Engelbrecht T, Neubert RHH, Goebel ASB (2010) New nanosized technologies for dermal and transdermal drug delivery. A review. J Biomed Nanotechnol 6: 511–528.

Schwarz J, Weisspapir M, Friedman D (1995) Enhanced transdermal delivery of diazepam by submicron emulsion (sme) creams. Pharm Res 12: 687–692.

Shafiq S, Shakeel F, Talegaonkar S, Ahmad F, Khar R, Ali M (2007) Development and bioavailability assessment of ramipril nanoemulsion formulation. Eur J Pharm Biopharm 66: 227–243.

Sølberg J, Ulrich NH, Krustrup D, Ahlström MG, Thyssen JP, Menné T, Bonefeld CM, Gadsbøll AØ, Balslev E, Johansen JD (2019) Skin tape stripping: Which layers of the epidermis are removed? Contact Dermatitis 80: 319–321.

Souto EB, Cano A, Martins-Gomes C, Coutinho TE, Zielinska A, Silva AM (2022) Review: Microemulsions and Nanoemulsions in Skin Drug Delivery. Bioengineering 9: 158.

Takada S, Naito S, Sonoda J, Miyauchi Y (2012) Noninvasive in vivo measurement of natural moisturizing factor content in stratum corneum of human skin by attenuated total reflection infrared spectroscopy. Appl Spectrosc 66: 26–32.

Talhouni AA, Alkrad JA, Al-Dabbagh MM, Abazid H, Hussein-Al-Ali SH (2019) Transdermal of atenolol via micro emulsions. Int J App Pharm 11: 164–171.

Tartaro G, Mateos H, Schirone D, Angelico R, Palazzo G (2020) Microemulsion microstructure(s): a tutorial review. Nanomaterials 10: 1657.

Tenjarla S (1999) Microemulsions: an overview and pharmaceutical applications. Crit Rev Ther Drug Carrier Syst 16: 461–521.

Valenta C, Schultz K (2004) Influence of carrageenan on the rheology and skin permeation of micro emulsion formulations. J. Control Release 95: 257–265.

Verdier-Sévrain S, Bonté F (2007) Skin hydration: a review on its molecular mechanisms. J Cosmet Dermatol 6: 75–82.

Zhang J, Michniak-Kohn B (2011) Investigation of micro emulsion microstructures and their relationship to transdermal permeation of model drugs: ketoprofen, lidocaine, and caffeine. Int J Pharm 421: 34–44.

Zhong FM, Yu CR, Luo C, Shoemaker Y, Li SQ, Xia JG (2009) Formation and characterisation of mint oil/S and CS/water micro emulsions. Food Chem 115: 539–544.

Zhou H, Yue Y, Liu G, Li Y, Zhang J, Gong Q, Yan Z, Duan M (2009) Preparation and characterization of a lecithin nanoemulsion as a topical delivery system. Nanoscale Res Lett 5: 224–230.

Zhu W, Guo C, Yu A, Cao F, Zhai G (2009) Microemulsion-based hydrogel formulation of penciclovir for topical delivery. Int J Pharm 378: 152–158.

Zidan AS, Kamal N, Alayoubi A, Seggel M, Ibrahim S, Rahman Z, Cruz CN, Ashraf M (2017) Effect of isopropyl myristate on transdermal permeation of testosterone from carbopol gel. J Pharm Sci 106: 1805–1803.

Zou Y, Maibach HI (2018) Dermal–epidermal separation methods: research implications. Arch Dermatol Res 310: 1–9.